

This is the author's final, peer-reviewed manuscript as accepted for publication (AAM). The version presented here may differ from the published version, or version of record, available through the publisher's website. This version does not track changes, errata, or withdrawals on the publisher's site.

# **Intracellular water – an overlooked drug target? Cisplatin impact in cancer cells probed by neutrons**

M.P.M. Marques, A.L.M. Batista de Carvalho,  
V. Garcia Sakai, L. Hatter  
and L.A.E. Batista de Carvalho

## **Published version information**

**Citation:** MPM Marques et al. "Intracellular water – an overlooked drug target? Cisplatin impact in cancer cells probed by neutrons." *Physical Chemistry Chemical Physics*, vol.19, no. 4 (2017): 2702-2713.

**doi:** [10.1039/C6CP05198G](https://doi.org/10.1039/C6CP05198G)

This version is made available in accordance with publisher policies. Please cite only the published version using the reference above.

This item was retrieved from **ePubs**, the Open Access archive of the Science and Technology Facilities Council, UK. Please contact [epubs@stfc.ac.uk](mailto:epubs@stfc.ac.uk) or go to <http://epubs.stfc.ac.uk/> for further information and policies.



PCCP

ARTICLE

## Intracellular Water – an Overlooked Drug Target? Cisplatin Impact in Cancer Cells Probed by Neutrons

M. P. M. Marques\*<sup>†a,b</sup>, A.L.M. Batista de Carvalho\*<sup>†a</sup>, V. Garcia Sakai<sup>c</sup>, L. Hatter<sup>d</sup> and L. A.E. Batista de Carvalho<sup>a</sup>

Background  
Received 00th January 20xx,  
Accepted 00th January 20xx

DOI: 10.1039/x0xx00000x

www.rsc.org/

The first neutron scattering study on human nucleated cells is reported, addressing the subject of solvent-slaving to a drug by probing intracellular water upon drug exposure. Inelastic and quasi-elastic neutron scattering spectroscopy with isotope labelling was applied for monitoring interfacial water response to the anticancer drug cisplatin, in the low prognosis human metastatic breast cancer cells MDA-MB-231. Optical vibrational data were also obtained for lyophilised cells. Concentration-dependent dynamical changes evidencing a progressive mobility reduction were unveiled between untreated and cisplatin-exposed samples, concurrent with variations in the native organisation of water molecules within the intracellular medium as a consequence of drug action. The results thus obtained yielded a clear picture of the intracellular water response to cisplatin and constitute the first reported experimental proof of a drug impact on the cytomatrix by neutron techniques. This is an innovative way of tackling a drug's pharmacodynamics, searching for alternative targets of drug action.

### Introduction

Water supports vital biochemical processes in a living organism, influencing key cellular functions such as protein folding and stability, enzyme catalysis, DNA packaging, molecular recognition, intracellular signalling, transport processes and cellular tolerance to freezing<sup>1-7</sup>. Actually, hydration is required for bioactivity, since it is essential for maintaining the functional structure of biomolecules. Within a biological system such as a cell, water structure and dynamics are known to be changed by the presence of metabolites or extrinsic entities (*e.g.* drugs), while in turn water properties are prone to affect the conformational behaviour and function of biomolecules, which are slaved to the variations occurring in their hydration shell<sup>5-13</sup>. The aqueous cytoplasm comprises a complex array of organised macromolecular structures, including skeletal elements and organelles, and dissolved solutes of various dimensions<sup>14-16</sup>, water amounting for about 80% of the total cell mass. The unique properties of water in the intracellular space have long been a matter of dispute, and

they have been found to determine the stiffness of the cytoplasm<sup>17</sup>. Dynamic labile H-bond networking, macromolecular crowding and confinement effects (by biomolecules and membranes of diverse physical-chemical nature) have been proposed to explain these distinctive molecular properties. Self-association through hydrogen bonding is a particularly important property, which is constantly changing as a consequence of the rotation of individual water molecules, as well as to accommodate the presence of solutes within the cellular milieu or to adapt to specific conditions (*e.g.* ionic strength, pH, temperature or pressure).

Because water provides the dynamical matrix in which all biochemical and biophysical processes occur, interference with its structural and dynamical characteristics is expected to have significant consequences at the functional level, and may even induce cell damage. Unravelling water behaviour within the cell, at the molecular level, is thus of key importance. Actually, even subtle changes in intracellular water may be the driving force to disrupt homeostasis and initiate a series of events leading to biomacromolecular dysfunction that can facilitate disease (*e.g.* cancer or neurological disorders)<sup>18</sup>. This concept is presently extended to the mode of action of pharmacological agents, which are likely to affect the inhomogeneous highly crowded cytoplasmic medium, with still unknown effects on cellular function. This is an innovative approach to better interpret pharmacodynamics (drug interaction with its pharmacological target), possibly unveiling secondary therapeutic targets, and attain an improved understanding of the drug's *in vivo* mode of action, helping to

<sup>a</sup> Unidade de I&D Quimica-Física Molecular, Dep. of Chemistry, R. Larga, 3004-535 Coimbra, Univ. Coimbra, Portugal

<sup>b</sup> Dep. Life Sciences, Univ. Coimbra, Calçada Martim de Freitas, 3000-456 Coimbra, Portugal

<sup>c</sup> ISIS Facility, STFC Rutherford Appleton Laboratory, Chilton, Didcot, OX 11 0QX, United Kingdom

<sup>d</sup> Research Complex at Harwell, STFC Rutherford Appleton Laboratory, Chilton, Didcot, OX 11 0FA, United Kingdom

† These authors contribute equally to this work.

Electronic Supplementary Information (ESI) available: Experimental procedures comprising: chemicals, cell culture and details on the optical vibrational spectroscopy spectrometers/data acquisition. See DOI: 10.1039/x0xx00000x

develop more effective therapies against cancer and optimise the use of presently available drugs.

The cell interior may be pictured as a gel-like structure, in which intracellular water is mostly confined and interacting with biomolecules and organelle surfaces – interfacial water – thus displaying properties that are significantly different to those of pure (extracellular) water. Nuclear magnetic resonance (NMR) has long been applied to investigate the intracellular hydrodynamics as a response to either external agents or abnormal physiological conditions<sup>19–26</sup>, as well as nonlinear optical spectroscopy techniques<sup>27–29</sup>. However, the NMR spatial and time scales (typically a few milliseconds) limits the results to average properties, and does not allow to discriminate the different dynamical contributions. Up to this date, a microscopic picture of cellular water has only been achieved by neutron scattering techniques, that have the ability to “see” proton positions, probing the space domain down to a few Angstroms at the nano- and picosecond time scales, thus yielding results not achievable by other methods. So far, these techniques have been applied to biomolecules such as proteins<sup>30–33</sup>, enzymes<sup>34</sup> and DNA<sup>35,36</sup>, as well as to more complex biological systems, namely *Artemia* shrimp cysts<sup>37</sup>, yeast cells<sup>38</sup>, human red blood cells<sup>25,39</sup>, extreme halophiles<sup>25,40</sup>, *Escherichia coli* bacteria<sup>25,41</sup> or stratum corneum<sup>42</sup>. In addition, molecular dynamics simulations of water–biomolecule interactions have been performed<sup>24,43,44</sup> in order to assist interpretation of the experimental data gathered for these samples (which is directly comparable to the theoretical results). Nevertheless, the major emphasis of these studies has been on the biomolecules rather than the water properties.

Incoherent inelastic neutron scattering spectroscopy (INS) is a particularly appropriate technique to tackle water in a biological matrix, since it is optimal for studying materials containing hydrogen atoms that have a scattering cross section (about 80 barns) which is much larger than for most other elements (at most *ca.* 5 barns). The neutron scattering cross-section of an element ( $\sigma$ ) is a characteristic of each isotope and independent of the chemical environment. During the scattering event, a fraction of the incoming neutron energy can be used to cause vibrational excitation, and the vibrational modes with the largest hydrogen displacements will dominate the spectrum. Therefore, INS will be particularly important in solids in which the molecular units are linked together by hydrogen close contacts (such as water) and the lowest-frequency vibrations are those expected to be most affected. The INS intensity of each vibrational transition is normally expressed in terms of the so-called dynamic structure factor  $S_i^*(Q, \nu_k)$ , which has the simplified expression, for a given atom

$$S_i^*(Q, \nu_k) = \frac{(Q^2 u_i^2) \sigma}{3} \exp\left(-\frac{Q^2 \alpha_i^2}{3}\right) \quad (1)$$

where  $Q$  ( $\text{\AA}^{-1}$ ) is the momentum transferred to the sample at a given scattering angle,  $\nu_k$  is the energy of a vibrational mode,  $u_i$  ( $\text{\AA}$ ) is the displacement vector of atom  $i$  in mode  $k$ ,  $\sigma$  is the neutron scattering cross section of the atom, and  $\alpha_i$  ( $\text{\AA}$ ) is

related to a mass-weighted sum of the displacements of the atom in all the vibrational modes. The exponential term,  $\exp[-(Q^2 \alpha_i^2)/3]$  is the Debye-Waller factor, that describes the attenuation of the neutron scattering process due to thermal motion. The harmonic frequencies (energies) of the vibrational modes correspond to eigenvalues, and the displacements to eigenvectors, of the dynamical matrix that can be calculated by theoretical methods (*e.g.* Density Functional Theory – Plane-Wave).

Quasi-elastic incoherent neutron scattering (QENS), in turn, analyses the incoherent (hydrogen-dominated) scattering signal within a meV energy transfer range, on a nanometer length scale (*ca.* 0.1–3 nm, corresponding to inter- and intramolecular distances) and a nano- to picosecond time scale (*ca.*  $10^{-9}$  –  $10^{-13}$  s). Hence, QENS is a method of choice for directly accessing different spatially resolved dynamical processes, from fast localised modes including vibrations and rotations to slower global translational motions. It is particularly suited for hydrogen-containing molecules, allowing to accurately probe water dynamics under different conditions in multi-component systems such as biological samples, thus helping to determine a relationship between dynamics and function<sup>30,45,46</sup>.

The QENS signal is detected as a broadening around the elastic line and is due to a variety of motions (which fall in the spectrometer’s time window). In a neutron scattering experiment, information on the molecular dynamics is obtained by measuring the dynamic structure factor,  $S(Q, \omega)$ , which represents the probability of an incident neutron to undergo a scattering event by transferring a momentum  $Q$  and an energy  $\omega$ . The corresponding experimental scattering function can be represented by,

$$S_{\text{measured}}(Q, \omega) = \exp\left(-\frac{\hbar\omega}{2kT}\right) R(Q, \omega) \otimes S(Q, \omega) \quad (2)$$

where  $\exp[-\hbar\omega/2kT]$  is a detailed balance factor, and  $R(Q, \omega)$  is a resolution function (experimentally obtained) which is convoluted with the scattering model ( $S(Q, \omega)$ ) that describes the dynamical behaviour of the sample (accounting for all the dynamical components of the system). In a hydrogenous sample,  $S(Q, \omega)$  is dominated by incoherent scattering, as the incoherent scattering cross section of an H atom is much greater than the coherent or incoherent scattering cross section of any other atom.  $S_{\text{inc}}(Q, \omega)$  corresponds to the self correlation function (incoherent dynamic structure factor) and is generally approximated as the convolution of vibrational, rotational and translational components which are assumed as independent motions:

$$S_{\text{inc}}(Q, \omega) = S_{\text{vib}}(Q, \omega) \otimes S_{\text{rot}}(Q, \omega) \otimes S_{\text{trans}}(Q, \omega) \quad (3)$$

Strictly in the elastic and quasielastic regions,

$$S_{\text{inc}}(Q, \omega) = \exp(-Q^2 \langle u^2 \rangle) [A_0(Q) \delta(\omega) + (1 - A_0(Q)) L(Q, \omega)] \quad (4)$$

where the exponential term is the Debye-Waller factor,  $A_0(Q) \delta(\omega)$  represents the elastic contribution due to motions slower than the longest observable time as defined by the energy resolution of the spectrometer, and the second term in the equation corresponds to the quasielastic component.

$S_{\text{inc}}(Q, \omega)$  directly provides time/space information on the system investigated: on the time scale of the dynamical processes (through the neutron energy transfer,  $\omega$ ), and on the spatial extent of these processes (from the momentum scattering transfer,  $Q$ ). Since the QENS data in the time-domain is represented by an exponential, it can be approximated in the energy domain by Lorentzian functions of different widths,  $\Gamma$  (full width at half-maximum,  $\text{FWHM}=2\times\text{HWHM}$  (half-width at half-maximum)), describing motions on different time scales:

$$L(x) = \frac{1}{\pi} \frac{\Gamma}{\Gamma^2 + \omega^2} \quad (5)$$

The behaviour of each  $\Gamma$  value with  $Q$  may subsequently be analysed to yield detailed information on each dynamical component contributing to the overall experimental QENS profile.

In the present study, inelastic and quasielastic neutron scattering techniques (INS and QENS) were used to probe water structure and dynamics (respectively) in human live cells, in the presence of the widely used antitumour drug cisplatin (*cis*-Pt(NH<sub>3</sub>)<sub>2</sub>Cl<sub>2</sub>)<sup>47-50</sup>. Indeed, apart from the well-known direct cytotoxic effect mediated by DNA conformational rearrangements<sup>51-53</sup>, cisplatin-induced changes in the intracellular water may have a noteworthy impact on vital biomolecules and affect cellular proliferation and viability. Pt(II) compounds constitute a specific class of metal-based anticancer agents, cisplatin, carboplatin and oxaliplatin being currently in clinical use<sup>51,52</sup> while numerous other Pt(II) complexes are being developed aiming at an increased antineoplastic activity coupled with a lower toxicity and a decreased acquired resistance<sup>54-63</sup>. The anticancer capacity of this kind of agents is recognised to be due to DNA severe damage through selective covalent binding of Pt(II) to the purine and pyrimidine bases (mainly adenine and guanine)<sup>53</sup>. These platinum-DNA adducts are formed following drug uptake into the cell and hydrolysis of the chloride ligands (sequential chloride by water substitution in the metal coordination sphere).

In what follows, we present INS and QENS data for human cells of invasive breast carcinoma (MDA-MB-231), to monitor their response to cisplatin as a function of drug concentration (8 to 20  $\mu\text{M}$ , for an exposure time of 48 hours previously determined to lead to a maximum drug effect (unpublished data)). Optical vibrational data (FTIR and Raman) were also obtained for lyophilised cell samples. The goal of this study was to directly probe water within intact human cancer cells, with a view to ascertain both structural and dynamical modifications upon drug incubation. This work, the first of its kind to be carried out using neutron techniques to probe live human nucleated cells (containing the whole array of cellular components), allowed to establish the suitability of neutron spectroscopy to unveil perturbations in intracellular water due to the presence of chemotherapeutic agents, as an innovative way of tackling a drug's pharmacodynamic behaviour. This will hopefully pave the way for further research on drug-induced effects on the intracellular medium, for conventional as well as

newly developed anticancer agents, aiming at assessing potential secondary pharmacological targets.

## Experimental

**Sample Preparation** The cell pellets (100 mg/1 cm<sup>3</sup>, ca. 5x10<sup>8</sup> cells *per* sample) were prepared by cell harvesting (through trypsinization) followed by repeated (2x) PBS washing and centrifugation (at 195 x g, for 15 min). PBS was used as an isotonic medium in order to avoid water exchange from the inside to the outside of the cell (leading to cell shrinkage). Under these conditions, the proportion of intracellular water was determined to be ca. 80% of the total cell weight (as expected for this type of neoplastic cells<sup>64</sup>) and the cell pellets contained less than 5% extracellular water (see quantification procedure below).

In order to remove this extracellular water component, the pellets (with and without drug) were washed with deuterated PBS by resuspension (1x), followed by centrifugation (at 195 x g) for 5 min which was repeated for 15 min after removing the first supernatant. These samples will be hereafter denominated PBS<sub>deut</sub>-washed cells (or simply washed cells), as opposed to the non-washed pellets. Lyophilised samples were also prepared, for both untreated and cisplatin-treated cells. After the neutron measurements, the integrity of the cell membrane was established by the Trypan blue assay. Cell viability assays were hindered by the unavoidable contamination upon sample handling during the neutron experiments (*e.g.* loading into the aluminium cans). Nevertheless, even considering cold-triggered denaturation of some cellular components (*e.g.* proteins) during spectral acquisition, the present study aims at a comparison between data obtained (at the same temperature) in the absence and presence of cisplatin – thus, cold-prompted effects (identical across all samples) will be cancelled out, only the perturbation due to the drug remaining.

**Quantification of Intracellular versus Extracellular Water in the Cell Pellets** The (intracellular:extracellular) water ratio was determined in the cell pellets, by comparing the weight of differently prepared samples: cell pellet immediately after harvesting and centrifugation (195 x g, for 10 min), containing both inter- and intracellular water ( $w_p$ ); cell pellet after drying in a dry atmosphere at 37 °C for ca. 3 hours, allowing for extracellular water to evaporate completely ( $w_D$ ); lyophilised cell pellet, comprising only the dehydrated cellular components ( $w_L$ ). Hence, ( $w_p-w_L$ ), ( $w_D-w_L$ ) and ( $w_p-[w_D-w_L]$ ) yielded the total water (inter+intracellular), the intracellular, and the extracellular water, respectively.

**Neutron Vibrational Spectroscopy** The neutron measurements were carried out at the ISIS Pulsed Neutron Source of the Rutherford Appleton Laboratory (<http://www.isis.stfc.ac.uk/>). The samples, containing ca. 100 mg/1 cm<sup>3</sup> of cell pellet (ca. 5x10<sup>8</sup> cells), were wrapped in aluminium foil sachets (which filled the beam) and loaded into flat thin walled aluminium cans.

In order to avoid slow ice crystal growth during freezing, that could extract water from cells leading to dehydration (an eventually to membrane disruption) the samples were plunged into liquid nitrogen for rapid freezing (*ca.* 1 s).

**Inelastic Neutron Scattering** INS spectra of MDA-MB-231 cells were obtained on the TOSCA spectrometer<sup>65</sup>, an indirect geometry time-of-flight broad range spectrometer ( $(\Delta E/E)$  *ca.* 1.25 %). To reduce the impact of the Debye-Waller factor (the exponential term in equation (1)) on the observed spectral intensity, the samples (in 0.2 mm-thick (4x4 cm) flat Al cans) were cooled to cryogenic temperature (*ca.* 10 K). Data were recorded in the energy range -24 to 4000  $\text{cm}^{-1}$ .

Apart from the drug-containing samples (8 and 20  $\mu\text{M}$ -cisplatin), untreated cellular controls were measured (for comparison when ascribing the cisplatin-induced changes), as well as cisplatin solutions (at all concentrations) in PBS, and PBS buffer (to assess the drug effect on the saline medium in the absence of the biological matrix). Lyophilised cells with and without drug (8  $\mu\text{M}$ ) were also analysed, with a view to identify the vibrational components due to biomolecules (mainly from proteins and DNA).

**Quasi-elastic Neutron Scattering** QENS spectra of MDA-MB-231 cells were acquired on the low-energy OSIRIS high-flux indirect-geometry time-of-flight spectrometer (<http://www.isis.stfc.ac.uk/instruments/osiris>)<sup>66</sup>, equipped with a newly installed beryllium filter<sup>67</sup>, and using the 002 reflection of the cooled pyrolytic graphite analyser bank (PG002 25Hz configuration) with a 25.4  $\mu\text{eV}$  energy resolution (FWHM). The data was recorded in the Q range 0.18 to 1.81  $\text{\AA}^{-1}$  (covering a 11° to 155° angular interval, for a total of 41 detectors), within the energy transfer window -0.8 to 2.0 meV. Drug-treated cells (8 and 20  $\mu\text{M}$ -cisplatin) and untreated cellular controls were measured, as well as PBS and cisplatin solutions in PBS. Both non-washed and PBS<sub>deut</sub>-washed samples were used, to accurately identify the contribution from bulk water.

In all cases 0.1 mm-thick (4x4 cm) flat Al cans were used, except for the PBS<sub>deut</sub>-washed samples and for PBS which were placed in 0.4 mm-thick (4x5 cm) Al containers (to allow for a higher amount of scatterer in the beam, still keeping to a 10% scatterer to reduce the possibility of multiple scattering). Spectra were run at 298 K, for *ca.* 20 h each. A vanadium sample (a purely incoherent elastic scatterer) was measured to define the instrument resolution and correct for detector efficiency.

**Data Analysis** The neutron data was reduced from raw time-of-flight signals into energy transfer spectra using the MANTID program (version 3.4.0<sup>68</sup>). The data acquired for both bulk water ( $\text{H}_2\text{O}$  and  $\text{D}_2\text{O}$ ) and PBS (non-deuterated and deuterated) was subtracted from that of the cell samples (respectively non-washed and PBS<sub>deut</sub>-washed), in order to better distinguish the features due to interfacial water.

QENS spectra were corrected for detector efficiency. Resolution functions were determined independently from calibration runs for vanadium (used for the non-cell containing samples), as well as for untreated non-washed and PBS<sub>deut</sub>-

washed cells (applied for the corresponding cell-containing samples).

Fitting of the QENS spectra was performed for the energy transfer range -0.8 to 2.0 meV, with the program DAVE (version 2.3, developed at the National Institute of Standards and Technology (NIST) Center for Neutron Research<sup>69</sup>). One Delta function (elastic component) and three Lorentzians (quasielastic contributions), plus an energy independent instrumental background, were necessary for an accurate representation of the system.

FWHM values were extracted from each of the Lorentzian functions representing the distinct dynamical components assigned to the system, yielding the translational diffusion coefficients ( $D_T$ ) and jump times ( $\tau_T$ ), as well as the correlation times for the localised motions of the cellular macromolecules ( $\tau_l$ ). For the translational Lorentzians, either a continuous diffusion (Fickian model,  $\Gamma=2DQ^2$ ) or a jump-reorientation mechanism were considered, the latter following the equation<sup>70-73</sup>:

$$\Gamma_T(Q) = \frac{D_T Q^2}{1 + D_T Q^2 \tau_T^{\text{jump}}} \quad (6)$$

where  $D_T$  represents the translational coefficient at temperature T and  $\tau_T^{\text{jump}}$  is the translational jump time (*i.e.* the mean residence time of a water molecule in each possible location).

## Results and Discussion

Water dynamics and structure were directly probed in intact human cancer cells of invasive breast carcinoma, in the presence of the widely used antineoplastic drug cisplatin. Several samples were investigated: (1) phosphate saline solution (PBS, both undeuterated and deuterated), as a good model for bulk water; (2) cell pellets, comprising biomolecules as well as extra- and intracellular water – non-washed cells; (3) cells in deuterated saline medium allowing to observe only intracellular water and biomolecules, as this PBS<sub>deut</sub>-washing procedure suppresses practically all the extracellular (bulk) water dynamical component by replacing the exchangeable hydrogens with poor scatterer deuterium atoms – PBS<sub>deut</sub>-washed cells; (4) cisplatin-exposed cells, including extra- and intracellular water and cellular constituents affected by the drug; (5) cisplatin-exposed cells in deuterated saline medium, containing intracellular water and cellular constituents affected by the drug – PBS<sub>deut</sub>-washed cisplatin-treated cells (or simply washed cisplatin-treated cells); (6) lyophilised cells, with and without drug, containing solely cytoplasmic biomolecules.

### Optical Vibrational Spectroscopy

Figure S1 (Electronic Supplementary Information, ESI) represents the optical vibrational data obtained (at room temperature) for two samples of lyophilised cells – both untreated and drug-treated (48 h incubation with 8  $\mu\text{M}$ -cisplatin), showing the main bands from the cellular metabolites (Tab. S1, Electronic Supplementary Information): (i) amide bands from the peptide bonds – I ( $\nu_{\text{C=O}}$ , at 1660  $\text{cm}^{-1}$ ),

II (60%  $\delta_{N-H}$  + 40%  $\nu_{C-N}$ , at 1550  $\text{cm}^{-1}$ ) and III (30%  $\delta_{N-H}$  + 40%  $\nu_{C-N}$ , centred at 1250  $\text{cm}^{-1}$ ); signals from the aromatic aminoacids (phenylalanine, tryptophan and tyrosine) at 1585, 1170, 1003 ( $\nu_s(\text{CC})_{\text{ring}}$ ) and 863  $\text{cm}^{-1}$ , and from phosphorylated proteins ( $\text{PO}_3^{2-}$  stretchings at ca. 980  $\text{cm}^{-1}$ ); (ii) typical features from the main cellular components, mostly lipids –  $\nu_{\text{CC}}$  (ca. 1130  $\text{cm}^{-1}$ ) and  $\delta_{\text{CH}_2/\text{CH}_3}$  (intense bands between 1400–1470  $\text{cm}^{-1}$ ); (iii) symmetric and antisymmetric (O–P–O) stretching modes from DNA and RNA (at 1090 and 1240  $\text{cm}^{-1}$ , respectively), and  $\nu(\text{CC})_{\text{ring}}$  from DNA's purine bases (e.g. 1320 to 1370  $\text{cm}^{-1}$ ).

Comparison of the infrared data from the control and drug-containing cells clearly demonstrates a marked effect of cisplatin on DNA and the protein cellular constituents (in accordance with previously reported studies for live MDA-MB-231 cells<sup>74</sup>), that is reflected by an almost complete disappearance of the peaks assigned to tyrosine (at 863  $\text{cm}^{-1}$ ) and the  $\text{PO}_3^{2-}$  symmetric stretching mode from proteins (at 980  $\text{cm}^{-1}$ ), coupled to a strong intensity decrease of the  $\nu_s(\text{O}-\text{P}-\text{O})$  signal from DNA (at ca. 1090  $\text{cm}^{-1}$ ), the latter being a recognised spectral biomarker of cell death<sup>75</sup>. The Raman spectra also expose the drug impact on the cellular chemical fingerprint: on DNA, supported by changes in the bands at ca. 720, 780, 920, 1170, 1314 and 1555  $\text{cm}^{-1}$  due to  $\nu(\text{CC})_{\text{ring}}$  modes from B-DNA bases and deoxyribose, and at 830  $\text{cm}^{-1}$  assigned to  $\nu(\text{O}-\text{P}-\text{O})_{\text{backbone}}$  (Tab. S1); on phospholipids (membranes), evidenced by the feature at 1033  $\text{cm}^{-1}$  clearly seen in the drug-treated sample; and on phenylalanine, which gives rise to a characteristic signal at 1003  $\text{cm}^{-1}$  that is enhanced in the cisplatin-containing samples, since drug binding to cellular proteins induces conformational rearrangements and unfolding leading to an increased exposure of aromatic aminoacids.

**INS** Neutron vibrational spectroscopy allows us to define the local structures of water molecules within the cell by comparing their vibrational signatures with known geometries, namely from ice in its different phases (since the neutron scattering measurements are performed at cryogenic temperatures). Interfacial water molecules in the vicinity of membranes and biomolecules within the cellular environment were reported (both by experimental data and molecular dynamics simulations) to yield different INS profiles relative to bulk water, in the translational (below ca. 300  $\text{cm}^{-1}$ ), librational (500 to 1000  $\text{cm}^{-1}$ ) and OH stretching (3200 to 3600  $\text{cm}^{-1}$ ) regions of the spectrum<sup>1,35,38,43</sup>. Figure 1 comprises the INS spectra presently measured (at 10 K) for human breast cancer cells: untreated and cisplatin-treated (8 and 20  $\mu\text{M}$ ) cell pellets and lyophilised cells, as well as PBS difference spectra (resulting from subtraction of the saline buffer to each of the cell pellet samples). Three distinct structural contributions could be identified, due to: 1) extracellular (bulk) water, yielding a broad and intense librational band at 540 to 1000  $\text{cm}^{-1}$  (identical to the H-bonded tetrahedral network of ice Ih), and a translational region comprising two peaks at 224 and 304  $\text{cm}^{-1}$ , assigned to intermolecular water-water hydrogen bonding<sup>76</sup>, as well as acoustic modes at 56 (very intense) and 155  $\text{cm}^{-1}$ ; 2) intracellular (interfacial) water, responsible for a

distinctive feature at ca. 560  $\text{cm}^{-1}$ ; 3) cellular components, clearly perceived in the lyophilised sample in the 1280–1500  $\text{cm}^{-1}$  range (centred at ca. 1370  $\text{cm}^{-1}$ , mainly arising from  $\text{CH}_2$  deformation modes of proteins, lipids and carbohydrates), 240 and 290  $\text{cm}^{-1}$  from proteins ( $\tau(\text{CH}_3)$ , partially overlapped with the water intramolecular H-bonding features) and 160  $\text{cm}^{-1}$  from membrane lipids ( $\tau(\text{CH}_3)$ ) (Tab. S1). Indeed, unlike the INS profile of the cell pellets, the spectrum of the lyophilised cells gave rise to INS peaks solely due to the biomolecules within the cell since these samples were devoid of both extra- and intracellular water. Comparison of this data for the lyophilised cells with and without cisplatin allowed to uncover a drug effect on DNA through the corresponding adenine and thymine  $\nu(\text{CC})_{\text{ring}}$  band at 728  $\text{cm}^{-1}$  (which was not observed in the treated sample, Figure 1).

A slight blue shift (from 552 to 556  $\text{cm}^{-1}$ ) was detected in the librational band peak between the spectrum of PBS (as a model for extracellular water) and the drug-free cell pellet, which is ascribed to an enhanced rigidity in the structure of interfacial water (within the crowded cytoplasm). Upon cisplatin incubation a marked change in the spectral pattern was observed, the librational band (540–1000  $\text{cm}^{-1}$ ) resembling the profile characteristic of low-density amorphous ice<sup>76</sup>, in accordance with a noteworthy decrease in the ordering of water molecules within the drug-containing cytoplasm. The contribution from intracellular water was clearly unveiled upon subtraction of PBS from the data measured for the cells, either untreated or cisplatin-treated, evidencing striking variations relative to bulk (extracellular) water as a consequence of modifications in the respective H-bonding network (Figure 1): 1) the broad librational 540–1000  $\text{cm}^{-1}$  band was substituted by a much narrower signal centred at 560  $\text{cm}^{-1}$ , ascribed to interfacial water, which was progressively reduced in intensity with increasing cisplatin concentration; 2) the features characteristic of H-bonded bulk water molecules were affected – the 224  $\text{cm}^{-1}$  translational peak decreased, while the 304  $\text{cm}^{-1}$  signal shifted to 293, 285 and 283  $\text{cm}^{-1}$  (more noticeably in the drug-exposed samples, as a direct function of cisplatin concentration); 3) the  $\delta(\text{CH}_2)$  signal at 1450  $\text{cm}^{-1}$  mainly due to the cellular lipid constituents disappeared, as a consequence of the recognised metabolic impact of this type of Pt(II)-based agents<sup>74</sup>, while a band was detected at ca. 1350  $\text{cm}^{-1}$ , assigned to  $\nu(\text{CC})_{\text{ring}}$  and  $\delta(\text{CH})$  modes from DNA (adenine and guanine) and proteins (particularly tryptophan). Subtraction of the data for the lyophilised cells from the cisplatin (8  $\mu\text{M}$ )-exposed cells (after PBS exclusion) yielded a double-difference spectrum which best revealed the vibrational features of confined (cytoplasmic) water in the presence of the drug, since the contributions from extracellular water and the cellular constituents (metabolites and biomolecules) were removed. Analysis of this spectral profile corroborates the assignment of the 560  $\text{cm}^{-1}$  signal to intracellular water.

These results plainly show that drug exposure induces structural changes in intracellular water H-bonding network which are mainly reflected in the librational region, as expected, since this is strongly dependent on proton ordering

defining the geometrical arrangement within the lattice<sup>35,76,77</sup>. In fact, the hydrogen bonds in confined intracellular water, known to display significantly longer lifetimes (5 to 10x)<sup>36,78</sup> than those occurring in unconstrained water, are proposed to be further changed by cisplatin, with a profound impact on the intrinsic dynamics of water molecules within the cell as to their ability to rotate, translate and interact with biomolecules (in their hydration layers). Several water structures displaying different H-bonding profiles, resembling some of the known ice phases studied so far<sup>76</sup>, may then coexist within the cell upon increasing cisplatin exposure – e.g. hexagonal (Ih) to low-density amorphous (LDA) ice-like geometries. Indeed, the drug-induced conformational changes in DNA and proteins are expected to affect these molecule's hydration patterns, this effect being assumed to propagate into the native hydrogen bond network of water in the highly packed cytoplasm (the average distance between macromolecules in an eukaryotic cell being ca. 2 nm<sup>16</sup>).

In conclusion, the intramolecular H-bond network characteristic of intracellular water appears to be disrupted by the presence of the antitumour drug, the average interaction of each H<sub>2</sub>O to four neighbouring molecules being changed to a distinct lattice organisation within the intracellular medium, which encompasses water–water and water–biomolecules hydrogen-type interactions. Actually, the librational profile observed in the INS spectra of cisplatin-exposed cells compares better with LDA or cubic (Ic) forms of ice than with the polycrystalline hexagonal geometry of water at cryogenic temperatures (ice Ih). This data is in accordance with previous INS and QENS studies on the structure of water associated with DNA<sup>35,36,79,80</sup> and yeast cells<sup>38</sup>.

**QENS** Quasi-elastic data was acquired in the OSIRIS spectrometer, that is sensitive to motions with time scales of the order of the picoseconds (ca. 4-200 ps, within a length interval of ca. 4-20 Å), optimal for the detection of intracellular water dynamics and still allowing to perceive local motions of the biological macromolecules in the cytosol. Nevertheless, discrimination between both types of motions is far from straightforward considering the diversity of entities present in the heterogeneous cellular system under observation: cellular components such as sugars, lipids, proteins and DNA (moving with similar time-scales) and the intracellular milieu comprising water molecules in different local environments – cytoplasmic (less constrained) water and hydration water (in the vicinity of biomolecules, strongly adsorbed at their surface).

Intracellular water dynamics was currently investigated in human breast cancer cells under different conditions, by measuring several samples (at 298 K): (i) phosphate buffered saline (PBS) and cisplatin-containing (8 μM) PBS, to assess a possible drug effect on the saline medium; (ii) cell pellets, both drug-free (control) and cisplatin-treated (8 and 20 μM); (iii) cell pellets washed with deuterated saline (apart from the non-washed samples), in order to minimise the bulk water component and accurately identify the contribution from intracellular water.

In these densely packed cell pellets the intracellular medium accounts for ca. 95% of the total water within the system (according to the quantification of intra- versus extracellular water in the samples, see Experimental Section). A good approximation to the scattering signal due to the extracellular water contribution (ca. 5%) may be visualised in the difference QENS profile of the non-washed cells minus the PBS<sub>deut</sub>-washed ones depicted in Figure 2(A) (profile in blue), which clearly evidences the attenuation of this component upon its deuteration ( $\sigma_{\text{inc}}(\text{D})=2.05$  versus  $\sigma_{\text{inc}}(\text{H})=80.26$  barns) that allows an improved detection of the contribution from the intracellular water. Therefore, the henceforth discussion is mostly based on the analysis of PBS<sub>deut</sub>-washed cell samples, which are dominated by intracellular water apart from cellular metabolites and biomolecules. In fact, washing with deuterated saline in the conditions previously described (see Experimental Section) is expected to lead to prompt deuteration of the extracellular water with a negligible impact on the intracellular medium. In addition, subtraction of the PBS data from the results obtained for these cell pellets was carried out, with a view to completely remove the reminiscent bulk water component and plainly show the contributions from the intracellular milieu (Figure 2(B)).

Exposure to cisplatin was found to induce a reduced flexibility in both non-washed and washed cells, reflected in the narrowing of the corresponding QENS profiles in a concentration-dependent way (Figure 3 (A) and (B)). This drug-prompted reduced mobility of intracellular water is consistent with a glassy form as opposed to a flexible state in drug-free cells. Hence, a dynamical transition is proposed to take place upon drug exposure, associated to the onset of translational diffusion and localised motions of the cellular macromolecules, from an intracellular water plasticity in untreated cells to a significantly higher rigidity upon drug administration. This transition from a flexible to a glassy state is suggested to involve jumping between sites of different energy within the intracellular confined space, in the time window of the spectrometer, and the onset of glassy dynamics was found to depend on drug concentration. Since the cisplatin solutions were prepared in PBS, the drug effect on the saline medium was also monitored, a slight narrowing of the QENS profile having been observed for the drug-containing deuterated PBS (Figure 3(C)).

Fitting of the QENS spectra was attained using one Delta function (elastic component) and three Lorentzians (quasielastic contributions) (Figure 4). In fact, two Lorentzian functions were found not to suffice for accurately fitting the experimental data acquired for the complex system under study (Figure S2, Electronic Supplementary Information). One Delta and three Lorentzians were thus used to represent three major dynamical components which are proposed to correspond to the following three populations: 1) very slow motions of the largest organelles and cytoskeleton within the cell, as well as global motions of the macromolecules (slower than the longest observable time defined by the spectrometer resolution), represented by the Delta function; 2) slow diffusion of the intracellular water molecules (Q-dependent

reorientations mediated by hydrogen bonds), represented by the two narrower Lorentzians, corresponding to two different regimes that we ascribe to two types of intracellular water – water in the vicinity of the biomolecules and water from the rest of the intracellular milieu, beyond the hydration shells (hereafter called hydration and cytoplasmic water, respectively); 3) internal localised motions of the macromolecules and/or fast rotation of the water molecules within the cellular medium (Q-independent), attributed to the broader Lorentzian function.

Fitting of the QENS profiles obtained for the PBS<sub>deut</sub>-washed samples (with and without cisplatin) allowed to probe biomolecules and intracellular water exclusively. The fitting parameters were analysed as a function of the wave vector transfer (Q). The full widths at half-maximum were extracted from the Lorentzian functions representing each of these quasielastic dynamical components, and their dependence on Q<sup>2</sup> provided information on the dynamical behaviour of the system, at the different conditions tested: the confined localised motions (broad Lorentzian) yielded a flat, Q-independent profile, while the non-localised translations of intracellular water (narrower Lorentzians) gave rise to Q-dependent functions (Figure 5).

Each of the motions taking place within the MDA-MB-231 cells may then be approximated by a different model, which was shown to be affected by deuteration of the extracellular medium and, to a higher degree, by the presence of cisplatin. The plots represented in Figure 5 for the translational motions of intracellular water (both in the cytoplasm and in hydration shells) correspond to one plausible scenario, that the authors think is the most biologically plausible, taking into account the knowledge available on the activation process and cytotoxic mechanism of cisplatin within the cell (covalent binding to biomolecular targets such as DNA, upon chloride hydrolysis). Overall, cytoplasmic water displayed a higher degree of freedom than hydration water, as anticipated in view of the interactions taking place between the biomolecules and the water molecules in the corresponding hydration layers, that are tightly organised and allow restricted motions. Regarding the translational motions of cytoplasmic water, a dynamical profile in accordance with a translational jump diffusion model was observed, with significantly restricted motions when going from untreated cells to PBS<sub>deut</sub>-washed samples exposed to cisplatin at increasing dosages (8 and 20 μM, Figure 5 (A)). The hydration water, in turn, displayed a somewhat distinct dynamical pattern, going from a restricted Fickian diffusion in the drug-free cells (where hydration layers are intact) to a purely translational jump behaviour for 20 μM-treated cells (where hydration shells are less ordered, Figure 5 (B)). Apart from a possible direct drug effect, this variation in the hydration water confinement upon cisplatin treatment is proposed to be mainly due to the drug-prompted reorientation of the cellular biomolecules (e.g. proteins<sup>81,82</sup>, DNA) causing a disturbance of their native structure and a consequent disruption of their highly organised hydration layers, leading to an enhanced degree of freedom of the respective water molecules that cannot interact as effectively

with the high percentage of exposed hydrophobic groups (despite the increase in the surface available for interaction). In fact, the conformational rearrangements of proteins and other cellular macromolecules were previously reported to be responsible for a dynamical heterogeneity within the corresponding hydration layers<sup>83,84</sup>. Overall, as anticipated, the anticancer drug was shown to have an impact on both the cytoplasmic medium and the hydration water, which, in turn, influence each other. Actually, the drug impact on hydration water (mediated by the biomolecules' rearrangement) is foreseen to spread to the surrounding water molecules in the cytoplasm (adding to the direct drug effect), and cisplatin's impact on the cytosol, in turn, will gradually extend to the neighbouring hydration layers.

Particularly interesting is the intermediate behaviour detected for both cytoplasmic and hydration water in the samples exposed to the lowest drug dosage (8 μM): the experimental data is fitted to a restricted Fickian diffusion at low Q, and to a jump reorientation mechanism in the high Q region (beyond Q=1.25 Å<sup>-1</sup>), each type of water population within the intracellular environment appearing to display different dynamical regimes, as if the cell was still adjusting to the presence of the drug. This can then be pictured as a transitional state of drug-induced disorganisation, in which neither the hydration nor the cytoplasmic water behave purely as such – the former is proposed to be partially detached from the macromolecules' surface, mixing with the outside water in the cytosol, while the latter becomes part of this more restricted environment around the cellular components. This dynamical change occurs for a distance of ca. 4 Å (that is within the boundaries of a biomolecule's hydration shell) – beyond this limit, water molecules display a cytoplasmic behaviour, and below they behave as more constrained hydration water.

Hence, upon a progressively higher degree of confinement to ca. 4 Å – from untreated non-washed to PBS<sub>deut</sub>-washed untreated and PBS<sub>deut</sub>-washed drug-containing cells – the dynamical profile of cytoplasmic water appears to be better adjusted by a translational jump model than by a simple Fickian diffusion. This jump reorientation or extended jump model (EJM)<sup>71-73</sup> was described to occur through a sequence of discrete large amplitude angular jumps involving an exchange of H-bond acceptors, as opposed to the Fickian-like continuous diffusive mechanism (either unrestricted or restricted) that proceeds *via* a sequence of infinitely small diffusive steps (according to  $\Gamma=2DQ^2$ ). In the translational jump model, the H-bond cleavage and the molecular reorientation take place concertedly and not successively as usually considered, and each time one of the approximately four H-bonds formed by a water molecule is exchanged, the molecule's centre of mass undergoes a translational shift. This reorientation process is therefore dependent on the local environment of the water molecules, and is anticipated to be affected by the presence of an extrinsic entity (such as a drug) in the intracellular medium. Moreover, when H-bonds are ruptured zones of higher density water are created (*i.e.* density is locally higher than the bulk)

which is expected to have an effect on the conformation (and therefore function) of neighbouring biomolecules.

The translational diffusion coefficients ( $D_T$ ), translational jump times ( $\tau_T$ ) and correlation times for the localised motions of the cellular macromolecules ( $\tau_L$ ), at each drug concentration tested, were extracted from the dynamical model considered for each case. The values thus obtained clearly reflected the effect of cisplatin on the intracellular medium. For the cells in deuterated saline medium (washed samples), the diffusion coefficients obtained for cytoplasmic water were consistent with an enhanced rigidity, in a concentration-dependent way:  $D_T^{298}=1.04\pm 0.05\times 10^{-5}$  vs  $0.19\pm 0.01\times 10^{-5}$   $\text{cm}^2\text{s}^{-1}$  and  $\tau_T^{298}=1.00\pm 0.10$  vs  $7.39\pm 1.16$  ps, for control and cisplatin/20  $\mu\text{M}$ -treated cells, respectively. For water within hydration shells, in turn, a reverse effect was observed (as previously discussed):  $D_T^{298}=0.03\pm 0.0004\times 10^{-5}$  vs  $1.39\pm 0.13\times 10^{-5}$   $\text{cm}^2\text{s}^{-1}$ , for control and cisplatin (20  $\mu\text{M}$ )-exposed samples. Regarding the correlation times for the localised motions of the cellular constituents quite high values were measured, as expected in view of the large dimensions of the biomolecules and the crowded intracellular environment in which they move:  $\tau_L^{298}=21.94\pm 0.04$ ,  $21.43\pm 0.04$  and  $18.12\pm 0.07$  ps for untreated and cisplatin-treated (8 and 20  $\mu\text{M}$ ), respectively. The  $\tau_L$  decrease detected upon drug-exposure, mainly in the presence of the highest cisplatin concentration (20  $\mu\text{M}$ ), may be justified by the drug-induced structural disruption of the intracellular water that will ease these localised motions of the macromolecular solutes.

These dynamical parameters obtained for MDA-MB-231 cells were compared with previously reported values for *Escherichia coli* bacteria<sup>25,41</sup>:  $D_T^{298}=1.04\pm 0.05\times 10^{-5}$  vs  $D_T^{301}=2.39\pm 0.05\times 10^{-5}$   $\text{cm}^2\text{s}^{-1}$  and  $\tau_T^{298}=1.00\pm 0.10$  vs  $\tau_T^{301}=1.54\pm 0.08$  ps, respectively for drug-free cancer cells and *E. coli*. Actually, while the results published for *E. coli* were not significantly different from those determined for pure water ( $D_T^{298}=2.3\times 10^{-5}$   $\text{cm}^2\text{s}^{-1}$ <sup>85</sup>), evidencing an intracellular water diffusion process similar to bulk water, the same was not verified in the currently probed human breast adenocarcinoma cells for which a considerably restricted intracellular water dynamics was observed (under identical conditions). This may be justified by the fact that eukaryotic cells have an extremely crowded cellular environment (macromolecular concentrations as high as 400  $\text{mg}\cdot\text{ml}^{-1}$  and distances among biomolecules of *ca.* 1 nm) as opposed to bacteria, leading to a much higher degree of confinement of intracellular water, its dynamics being better adjusted by a jump diffusion model than by a simple Fickian diffusion. Furthermore, the translational diffusion coefficients presently obtained for cytoplasmic water in the breast cancer cells exposed to cisplatin are one order of magnitude lower than the value obtained by QENS for extreme halophiles (in which the high salt concentration leads to a significant reduced mobility of *ca.* 76% of intracellular water)<sup>40</sup> –  $D_T^{298}=0.19\pm 0.01\times 10^{-5}$  (cisplatin-20  $\mu\text{M}$ ) vs  $D_T^{285}=1.29\times 10^{-5}$   $\text{cm}^2\text{s}^{-1}$ , respectively.

## Conclusions

The present study was based on the assumption that in human cells the behaviour of cytoplasmic water (both structural and dynamical) determines not only the conformation and function of biomolecules (primarily through their hydration shells), but may also be tamed by the cellular constituents – the cellular macromolecules “dance” to the tune of intracellular water and *vice versa*, in a twofold, intertwined, process. Hence, any effect that a drug may exert on vital macromolecules (such as DNA or proteins) will also have a predictable impact on intracellular water, with consequences on cellular function, thus constituting a potential secondary pharmacological target. The reported combined inelastic and quasi-elastic neutron scattering spectroscopy work allowed to establish the feasibility of these techniques to probe complex macromolecular systems such as human cells, with a view to gain a deeper insight into confined intracellular water and monitor perturbations to its structural and dynamical behaviour (*e.g. via* interference with its native H-bonding network) due to the presence of external agents such as chemotherapeutic drugs. A quite accurate picture was attained regarding the structural features and microscopic diffusion of water molecules within intact human breast cancer cells in the absence and presence of a DNA-binding anticancer agent (cisplatin, at 8 and 20  $\mu\text{M}$ ).

The results thus obtained revealed a clear picture of the intracellular water response to a drug, evidencing clear differences relative to non-treated cells, therefore disclosing a clear impact of cisplatin on the cytomatrix. Coupled to different structural properties, mainly reflected in the librational region of the INS spectra, this antitumour agent was found to affect the dynamic state of intracellular water, rendering it different from bulk water and also from the cellular medium in drug-free samples, this effect being concentration-dependent (increasing from [cisplatin]=8 to 20  $\mu\text{M}$ ). Diffusion of intracellular water molecules is known to be restricted due to confinement within the crowded cytoplasmic environment coupled to strong interactions with biomolecules and membranes (structured water in hydration shells). In the presence of cisplatin, these effects were found to be enhanced due to the drug's effect on DNA and subsequently on other cellular constituents (*e.g.* proteins and membranes), disrupting their folded native conformation and thus increasing disorder and crowding in the cellular milieu with a significant impact on water properties. Intracellular water molecules with distinct structural and dynamical profiles – from the hydration shell around biomolecules (hydration water) and from the aqueous intracellular medium (cytoplasmic water) – could be discriminated by QENS. Both were found to be affected by the presence of the antitumour drug, a biologically reasonable interpretation of the data being presently suggested: while cytoplasmic water showed a progressively restrained dynamics upon cisplatin exposure (in a concentration-dependent way), the hydration shells became more ordered in the presence of 8  $\mu\text{M}$ -cisplatin and were prompted to a more mobile state for 20  $\mu\text{M}$ -cisplatin, as the biomolecules' native structure was more severely disrupted. This marked change in the dynamical profile of hydration water in the presence of a high drug

concentration is suggested to be a consequence of the drastic drug-triggered reorganisation of the intracellular macromolecules (into a nonfunctional conformation). Regarding cytoplasmic water, cisplatin apparently behaves as a kosmotropic (structure-making) solute<sup>86</sup>, which may be related to the significant increase in chloride ion concentration within the intracellular medium owing to drug hydrolysis (activation step).

To this date, reduced mobility of cellular water on an atomic scale had only been detected in yeast cells at cryogenic temperatures<sup>38</sup>, in low-hydrated *Artemia* shrimp cysts<sup>37</sup> or in extreme halophiles<sup>25,40</sup>, but never in eukaryotic cells. To the best of the authors' knowledge this is the first study of the kind carried out in human cells. In fact, distinct behaviours are likely to emerge between different types of cells, e.g. prokaryotic *versus* eukaryotic, namely arising from the presence of particular constituents in the latter (such as the cytoskeleton and the nucleus). Accordingly, the difference in atomic-scale viscosity presently unveiled for the intracellular environment in human cancer cells relative to pure water and to the QENS data reported for *E. coli* bacteria<sup>25,41</sup> is well justified, attending to the significantly higher crowding of the eukaryotic cells' cytoplasm. Actually, in bacteria, intracellular water beyond the hydration shells of macromolecules and membranes may flow as freely as bulk water, while in *Artemia* shrimp cysts<sup>37</sup> and extreme halophiles<sup>25,40</sup> a second intracellular water component was detected with a significantly slowed down translational diffusion, consonant to the present results for human cancer cells in the presence of a chemotherapeutic agent.

This study is an innovative way of tackling a drug's pharmacodynamics, searching for additional (and possibly ancillary) targets of drug action with a view to improve chemotherapeutic efficiency without increased deleterious side effects. The successful results already gathered pave the way for further work on drug impact on intracellular water, for conventional as well as newly developed anticancer agents. Whether this is a cell-specific effect still remains to be clarified (by monitoring distinct types of cancer cells), as well as the influence of water exchange kinetics across the cell membrane. These studies are expected to lead to a better understanding of the *in vivo* mode of action of antitumour agents used daily in the clinic, at a molecular level, providing valuable clues for the rational design of improved drugs, particularly polynuclear Pt(II)- and Pd(II)-polyamine cisplatin-like chelates which have been studied by the authors in the last decade.

## Acknowledgements

The authors acknowledge financial support from the Portuguese Foundation for Science and Technology – UID/MULTI/00070/2013, PhD fellowship SFRH/BD/72851/2010 and Project PTDC/QEQ-MED/1890/2014 (within Project 3599 – to Promote Scientific Production and Technological Development as well as the formation of thematic networks/3599-PPCDT – jointly financed by the European

Community Fund FEDER). The STFC Rutherford Appleton Laboratory is thanked for access to neutron beam facilities. The neutron work was supported by the European Commission under the 7<sup>th</sup> Framework Programme through the Key Action: Strengthening the European Research Area, Research Infrastructures (contract n°: CP-CSA\_INFRA-2008-1.1.1 Number 226507-NMI3). The authors are grateful to Dr. Pedro Vaz and Dr. Svemir Rudic for TOSCA instrumental support and to Dr. Franz Demmel for helpful scientific discussions.

## References

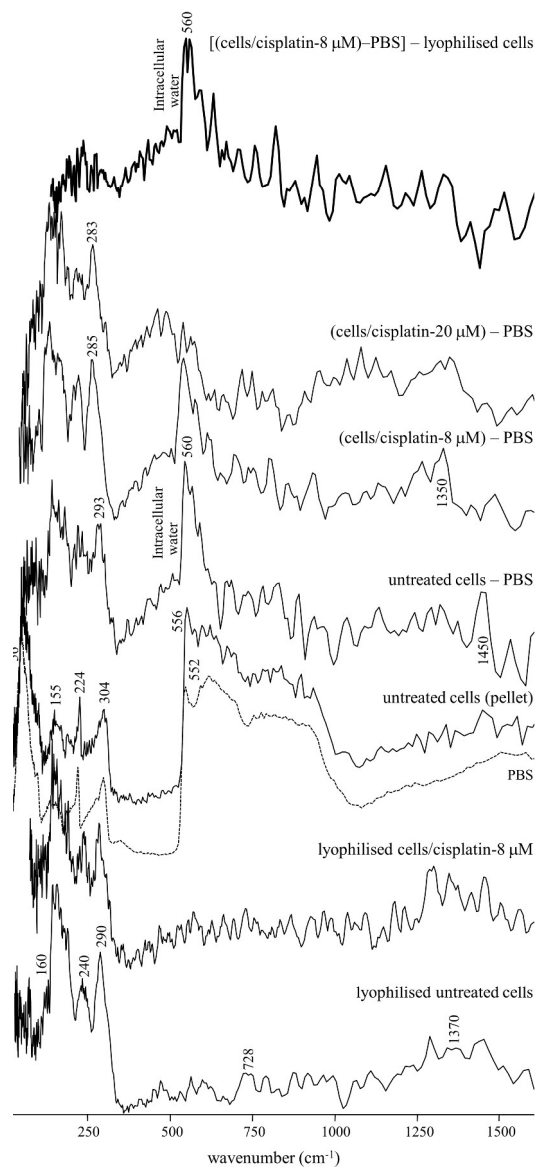
1. S. V. Ruffle, I. Michalarias, J. C. Li and R. C. Ford, *J Am Chem Soc*, 2002, 124, 565-569.
2. D. Le Bihan, *Phys Med Biol*, 2007, 52, R57-R90.
3. K. Wood, M. Plazanet, F. Gabel, B. Kessler, D. Oesterhel, D. J. Tobias, G. Zaccai and M. Weik, *Proc Natl Acad Sci USA*, 2007, 104, 18049-18054.
4. P. Ball, *Chem Rev*, 2008, 108, 74-108.
5. A. P. Sokolov, J. H. Roh, E. Mamontov and V. G. Sakai, *Chem Phys*, 2008, 345, 212-218.
6. E. Mamontov and X. Q. Chu, *Phys Chem Chem Phys*, 2012, 14, 11573-11588.
7. K. Luby-Phelps, *Mol Biol Cell*, 2013, 24, 2593-2596.
8. P. Mentre, *Cell Mol Biol*, 2001, 47, 709-715.
9. P. W. Fenimore, H. Frauenfelder, B. H. McMahon and F. G. Parak, *Proc Natl Acad Sci USA*, 2002, 99, 16047-16051.
10. S. K. Pal, J. Peon, B. Bagchi and A. H. Zewail, *J Phys Chem B*, 2002, 106, 12376-12395.
11. P. W. Fenimore, H. Frauenfelder, B. H. McMahon and R. D. Young, *Proc Natl Acad Sci USA*, 2004, 101, 14408-14413.
12. W. Doster and M. Settles, *BBA-Proteins Proteomics*, 2005, 1749, 173-186.
13. H. Frauenfelder, G. Chen, J. Berendzen, P. W. Fenimore, H. Jansson, B. H. McMahon, I. R. Stroe, J. Swenson and R. D. Young, *Proc Natl Acad Sci USA*, 2009, 106, 5129-5134.
14. J. Spitzer, *Microbiol Mol Biol Rev*, 2011, 75, 491-+.
15. M. Tabaka, T. Kalwarczyk, J. Szymanski, S. Hou and R. Holyst, *Front Phys*, 2014, 2.
16. F. X. Theillet, A. Binolfi, T. Frembgen-Kesner, K. Hingorani, M. Sarkar, C. Kyne, C. G. Li, P. B. Crowley, L. Gierasch, G. J. Pielak, A. H. Elcock, A. Gershenson and P. Selenko, *Chem Rev*, 2014, 114, 6661-6714.
17. G. Lenormand, E. Millet, C. Y. Park, C. C. Hardin, J. P. Butler, N. I. Moldovan and J. J. Fredberg, *Phys Rev E*, 2011, 83.
18. R. M. Davidson, A. Lauritzen and S. Seneff, *Entropy-Switz*, 2013, 15, 3822-3876.
19. S. Hortelano, M. L. Garcia-Martin, S. Cerdan, A. Castrillo, A. M. Alvarez and L. Bosca, *Cell Death Differ*, 2001, 8, 1022-1028.
20. E. Smouha and M. Neeman, *Magn Reson Med*, 2001, 46, 68-77.
21. T. Yamada, *Cell Mol Biol*, 2001, 47, 925-933.
22. L. Zhao, C. D. Kroenke, J. Song, D. Piwnica-Worms, J. J. H. Ackerman and J. J. Neil, *NMR Biomed*, 2008, 21, 159-164.
23. I. Aslund and D. Topgaard, *J Magn Reson*, 2009, 201, 250-254.
24. J. Qvist, E. Persson, C. Mattea and B. Halle, *Farad Discuss*, 2009, 141, 131-144.

## ARTICLE

## PCCP

25. M. Jasnin, A. Stadler, M. Tehei and G. Zaccai, *Phys Chem Chem Phys*, 2010, 12, 10154-10160.
26. C. S. Springer, X. Li, L. A. Tudorica, K. Y. Oh, N. Roy, S. Y. C. Chui, A. M. Naik, M. L. Holtorf, A. Afzal, W. D. Rooney and W. Huang, *NMR Biomed*, 2014, 27, 760-773.
27. E. O. Potma, W. P. de Boeij and D. A. Wiersma, *Biophys J*, 2001, 80, 3019-3024.
28. E. O. Potma, W. P. de Boeij, P. J. M. van Haastert and D. A. Wiersma, *Proc Natl Acad Sci USA*, 2001, 98, 1577-1582.
29. B. Born, S. J. Kim, S. Ebbinghaus, M. Gruebele and M. Havenith, *Farad Discuss*, 2009, 141, 161-173; discussion 175-207.
30. W. Doster, S. Cusack and W. Petry, *Nature*, 1989, 337, 754-756.
31. S. Dellerue and M. C. Bellissent-Funel, *Chem Phys*, 2000, 258, 315-325.
32. D. Russo, P. Baglioni, E. Peroni and J. Teixeira, *Chem Phys*, 2003, 292, 235-245.
33. R. E. Lechner, J. Fitter, N. A. Dencher and T. Hauss, *Physica B*, 2006, 385-86, 835-837.
34. A. V. Goupillamy, J. C. Smith, J. Yunoki, S. F. Parker and M. Kataoka, *J Am Chem Soc*, 1997, 119, 9268-9273.
35. I. A. Beta, A. I. Kolesnikov, I. Michalarias, G. L. Wu, R. C. Ford and J. C. Li, *Can J Phys*, 2003, 81, 367-371.
36. I. A. Beta, I. Michalarias, R. C. Ford, J. C. Li and M. C. Bellissent-Funel, *Chem Phys*, 2003, 292, 451-454.
37. E. C. Trantham, H. E. Rorschach, J. S. Clegg, C. F. Hazlewood, R. M. Nicklow and N. Wakabayashi, *Biophys J*, 1984, 45, 927-938.
38. R. C. Ford, S. V. Ruffle, A. J. Ramirez-Cuesta, I. Michalarias, I. Beta, A. Miller and J. C. Li, *J Am Chem Soc*, 2004, 126, 4682-4688.
39. A. M. Stadler, J. P. Embs, I. Digel, G. M. Artmann, T. Unruh, G. Buldt and G. Zaccai, *J Am Chem Soc*, 2008, 130, 16852-16853.
40. M. Tehei, B. Franzetti, K. Wood, F. Gabel, E. Fabiani, M. Jasnin, M. Zamponi, D. Oesterheld, G. Zaccai, M. Ginzburg and B. Z. Ginzburg, *Proc Natl Acad Sci USA*, 2007, 104, 766-771.
41. M. Jasnin, M. Moulin, M. Haertlein, G. Zaccai and M. Tehei, *EMBO Rep*, 2008, 9, 543-547.
42. J. Pieper, G. Charalambopoulou, T. Steriotis, S. Vasenkov, A. Desmedt and R. E. Lechner, *Chem Phys*, 2003, 292, 465-476.
43. S. Pal, S. Balasubramanian and B. Bagchi, *Phys Rev E*, 2003, 67.
44. D. J. Tobias, N. Sengupta and N. Tarek, *Farad Discuss*, 2009, 141, 99-116.
45. R. E. Lechner and S. Longeville, in *Neutron Scattering in Biology: Techniques and Applications*, eds. J. Fitter, T. Gutberlet and J. Katsaras, Springer, Berlin, 2006, DOI: 10.1007/3-540-29111-3\_16, ch. 16, pp. 355-397.
46. A. Frolich, F. Gabel, M. Jasnin, U. Lehnert, D. Oesterheld, A. M. Stadler, M. Tehei, M. Weik, K. Wood and G. Zaccai, *Farad Discuss*, 2009, 141, 117-130.
47. B. Rosenberg, L. Vancamp and T. Krigas, *Nature*, 1965, 205, 698-699.
48. B. Rosenberg, L. VanCamp, J. E. Trosko and V. H. Mansour, *Nature*, 1969, 222, 385-386.
49. L. A. E. Batista de Carvalho, M. P. M. Marques, C. Martin, S. F. Parker and J. Tomkinson, *Chemphyschem*, 2011, 12, 1334-1341.
50. M. P. M. Marques, R. Valero, S. F. Parker, J. Tomkinson and L. A. E. B. de Carvalho, *J Phys Chem B*, 2013, 117, 6421-6429.
51. D. Wang and S. J. Lippard, *Nat Rev Drug Discov*, 2005, 4, 307-320.
52. J. Reedijk, *Pure Appl Chem*, 2011, 83, 1709-1719.
53. M. P. M. Marques, D. Gianolio, G. Cibin, J. Tomkinson, S. F. Parker, R. Valero, R. P. Lopes and L. A. E. B. de Carvalho, *Phys Chem Chem Phys*, 2015, 17, 5155-5171.
54. M. P. M. Marques, T. Girao, M. C. P. De Lima, A. Gameiro, E. Pereira and P. Garcia, *Biochim Biophys Acta-Mol Cell*, 2002, 1589, 63-70.
55. L. J. Teixeira, M. Seabra, E. Reis, M. T. G. da Cruz, M. C. P. de Lima, E. Pereira, M. A. Miranda and M. P. M. Marques, *J Med Chem*, 2004, 47, 2917-2925.
56. L. Kelland, *Nat Rev Cancer*, 2007, 7, 573-584.
57. R. Tummala, P. Diegelman, S. M. Fiuza, L. A. E. B. De Carvalho, M. P. M. Marques, D. L. Kramer, K. Clark, S. Vujcic, C. W. Porter and L. Pendyala, *Oncol. Rep.*, 2010, 24, 15-24.
58. N. P. Farrell, *Curr Top Med Chem*, 2011, 11, 2623-2631.
59. S. Komeda, *Metallomics*, 2011, 3, 650-655.
60. S. Komeda, T. Moulai, M. Chikuma, A. Odani, R. Kipping, N. P. Farrell and L. D. Williams, *Nucleic Acids Res*, 2011, 39, 325-336.
61. M. P. M. Marques, *ISRN Spectrosc.*, 2013, 2013, 29.
62. T. M. Silva, S. Andersson, S. K. Sukumaran, M. P. Marques, L. Persson and S. Oredsson, *Plos One*, 2013, 8.
63. T. M. Silva, S. M. Fiuza, M. P. M. Marques, L. Persson and S. Oredsson, *Amino Acids*, 2014, 46, 339-352.
64. A. J. Fenn, in *Breast Cancer Treatment by Focused Microwave Thermotherapy*, Jones and Bartlett Publishers, Sudbury, Massachusetts, 2007.
65. S. F. Parker, C. J. Carlile, T. Pike, J. Tomkinson, R. J. Newport, C. Andreani, F. P. Ricci, F. Sacchetti and M. Zoppi, *Physica B*, 1997, 241, 154-156.
66. M. T. F. Telling and K. H. Andersen, *Phys Chem Chem Phys*, 2005, 7, 1255-1261.
67. F. Demmel, D. McPhail, J. Crawford, D. Maxwell, K. Pokhilchuk, V. Garcia-Sakai, S. Mukhopadhyay, M. T. F. Telling, F. J. Bermejo, N. T. Skipper and F. Fernandez-Alonso, *Epj Web Conf*, 2015, 83.
68. O. Arnold, J. C. Bilheux, J. M. Borreguero, A. Buts, S. I. Campbell, L. Chapon, M. Doucet, N. Draper, R. F. Leal, M. A. Gigg, V. E. Lynch, A. Markyarsen, D. J. Mikkelsen, R. L. Mikkelsen, R. Miller, K. Palmen, P. Parker, G. Passos, T. G. Perring, P. F. Peterson, S. Ren, M. A. Reuter, A. T. Savici, J. W. Taylor, R. J. Taylor, R. Tolchenoy, W. Zhou and J. Zikoysky, *Nucl Instrum Methods Phys Res Sect A-Accel Spectrom Dect Assoc Equip*, 2014, 764, 156-166.
69. R. T. Azuah, L. R. Kneller, Y. M. Qiu, P. L. W. Tregenna-Piggott, C. M. Brown, J. R. D. Copley and R. M. Dimeo, *J Res Natl Inst Stand Technol*, 2009, 114, 341-358.
70. J. J. Ullo, *Phys Rev A*, 1987, 36, 816-826.
71. D. Laage and J. T. Hynes, *Science*, 2006, 311, 832-835.
72. D. Laage and J. T. Hynes, *J Phys Chem B*, 2008, 112, 14230-14242.
73. D. Laage, *J Phys Chem B*, 2009, 113, 2684-2687.
74. A. L. M. Batista de Carvalho, M. Pilling, P. Gardner, J. Doherty, G. Cinque, K. Wehbe, C. Kelley, L. A. E. Batista de Carvalho and M. P. M. Marques, *Farad Discuss*, 2016, 187, 273-298.

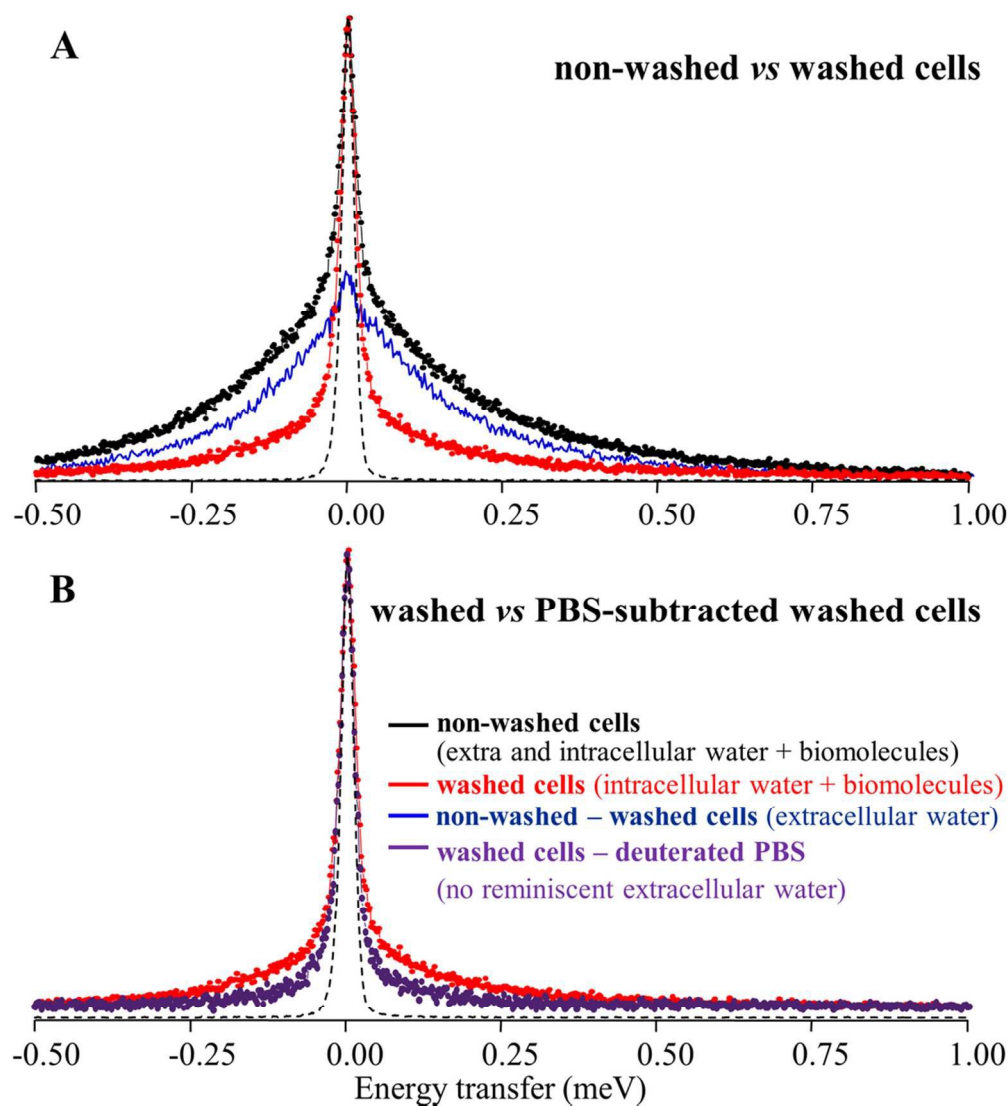
75. I. Notinger, S. Verrier, S. Haque, J. M. Polak and L. L. Hench, *Biopolymers*, 2003, 72, 230-240.
76. J. C. Li, *J Chem Phys*, 1996, 105, 6733-6755.
77. H. Fukazawa and M. Shinji, *Physics of Ice Core Records*, 2000, 25-42.
78. S. Balasubramanian, S. Pal and B. Bagchi, *Phys Rev Lett*, 2002, 89, 115505.
79. I. Michalarias, I. Beta, R. Ford, S. Ruffle and J. C. Li, *Appl Phys A-Mater Sci Process*, 2002, 74, S1242-S1244.
80. I. Michalarias, I. A. Beta, J. C. Li, S. Ruffle and R. Ford, *J Mol Liq*, 2002, 101, 19-26.
81. B. Born, S. J. Kim, S. Ebbinghaus, M. Gruebele and M. Havenith, *Farad Discuss*, 2009, 141, 161-173.
82. A. M. Stadler, F. Demmel, J. Ollivier and T. Seydel, *Phys Chem Chem Phys*, 2016, 18, 21527-21538.
83. S. Ebbinghaus, S. J. Kim, M. Heyden, X. Yu, U. Heugen, M. Gruebele, D. M. Leitner and M. Havenith, *Proc Natl Acad Sci USA*, 2007, 104, 20749-20752.
84. A. C. Fogarty and D. Laage, *J Phys Chem B*, 2014, 118, 7715-7729.
85. M. C. Bellissent-Funel, S. H. Chen and J. M. Zanotti, *Phys Rev E*, 1995, 51, 4558-4569.
86. P. Ball and J. E. Hallsworth, *Phys Chem Chem Phys*, 2015, 17, 8297-8305.



INS spectra (at 10 K) of MDA-MB-231 cells (pellet and lyophilized samples), both untreated and cisplatin-treated.

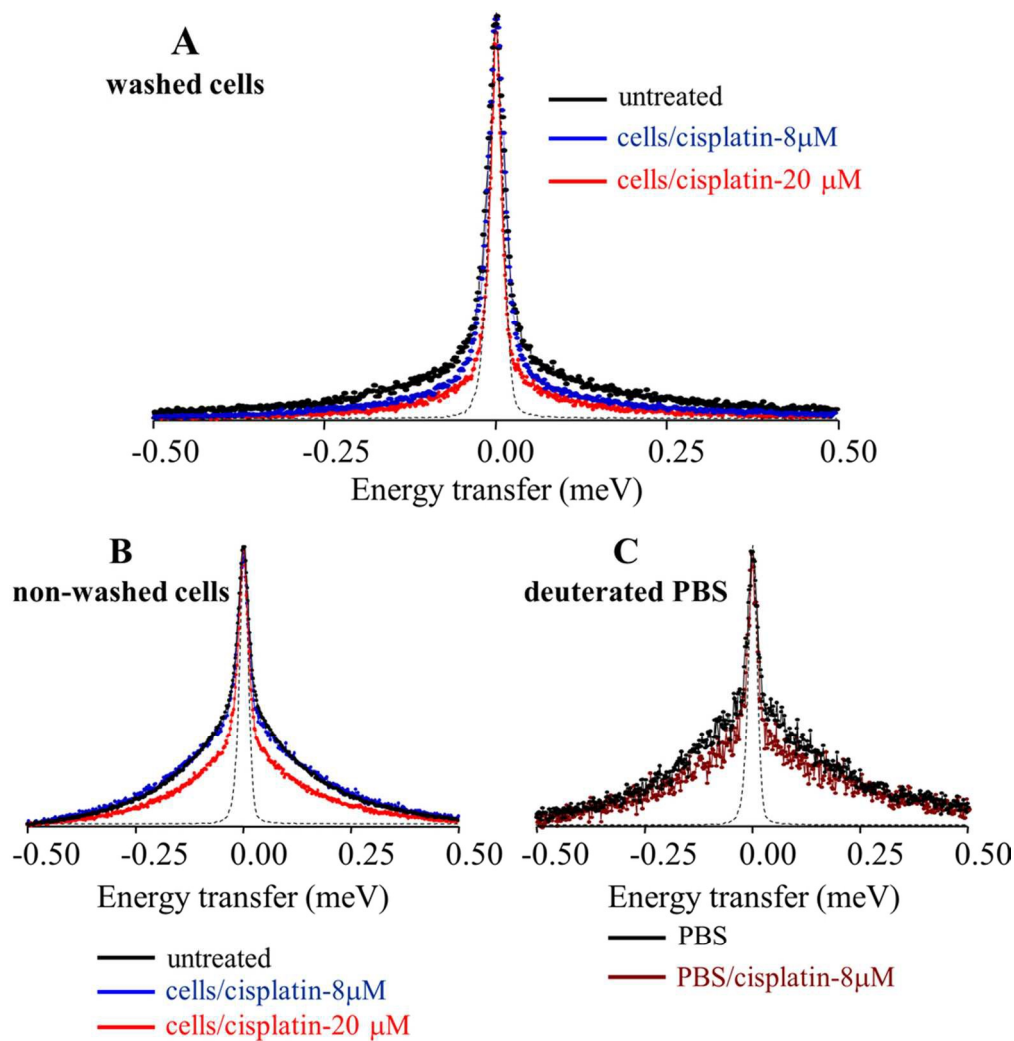
Figure 1

199x459mm (300 x 300 DPI)



QENS spectra (298 K) at  $Q=1.079 \text{ \AA}^{-1}$ , measured for untreated MDA-MB-231 cells: (A) Non-washed versus PBSdeut-washed cells. (B) Washed versus PBS-subtracted washed cells.!! † (Spectra were normalized to maximum peak intensity. The dashed line represents the instrument resolution, as measured by a standard vanadium sample).

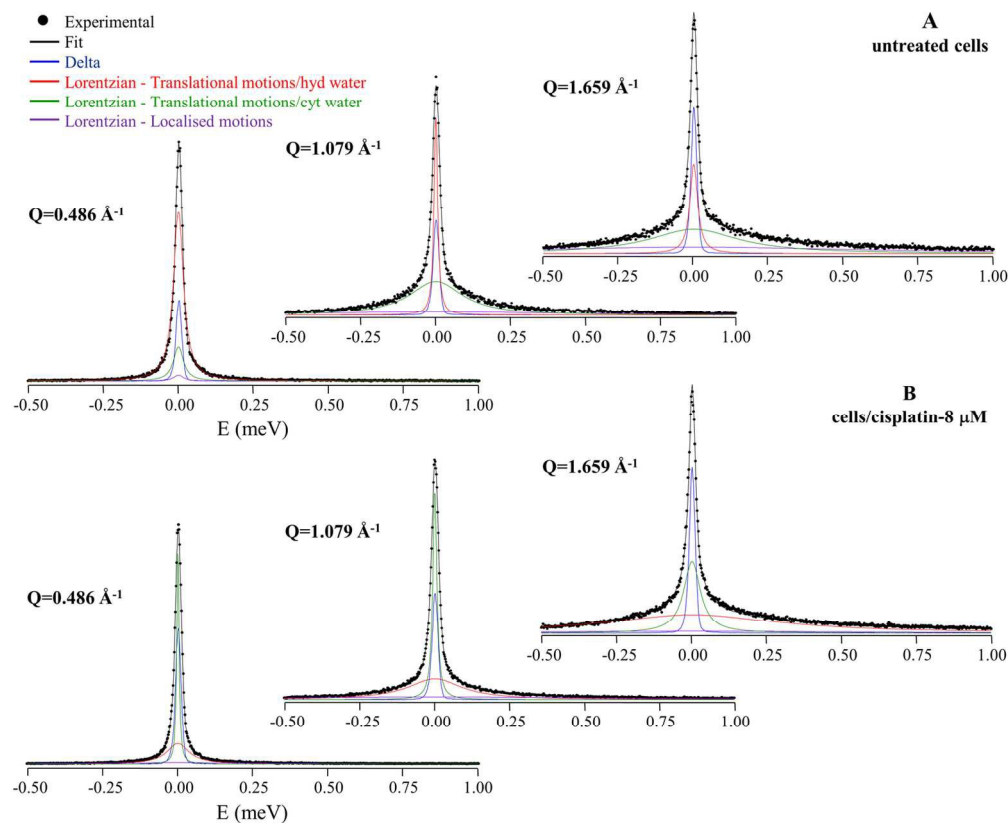
Figure 2  
94x103mm (300 x 300 DPI)



QENS spectra (298 K) at  $Q=1.079 \text{ \AA}^{-1}$ , measured for MDA-MB-231 cells and PBS, with and without cisplatin: (A) Cells in deuterated saline medium (washed). (B) Non-washed cells. (C) Deuterated saline medium.!! + (Spectra were normalized to maximum peak intensity. The dashed line represents the instrument resolution, as measured by a standard vanadium sample).

Figure 3

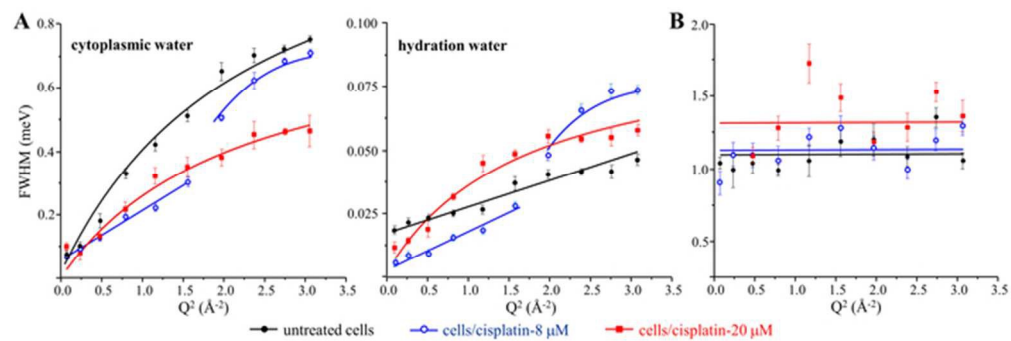
90x93mm (300 x 300 DPI)



QENS spectra (298 K) for untreated (A) and cisplatin-treated/8  $\mu\text{M}$  (B) MDA-MB-231 cells, in deuterated saline medium (washed), fitted using three Lorentzian and one Delta functions, at some typical Q values.

Figure 4

139x115mm (300 x 300 DPI)



Variation of the full widths at half-maximum (FWHM) with  $Q^2$  for untreated and cisplatin-treated (8 and 20  $\mu\text{M}$ ) MDA-MB-231 cells in deuterated saline medium (washed), at 298 K: (A) Lorentzian functions representing the translational motions of intracellular water – cytoplasmic and hydration water. (B) Lorentzian function representing the internal localized motions within the cell.

Figure 5

60x19mm (300 x 300 DPI)